

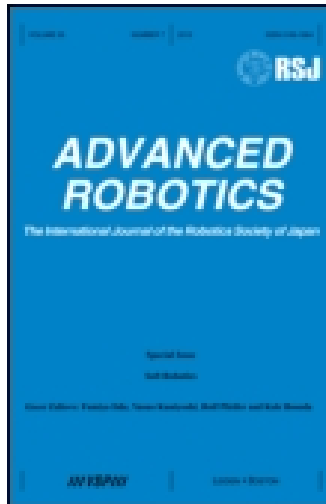
This article was downloaded by: [University of Central Florida]

On: 19 February 2015, At: 14:28

Publisher: Taylor & Francis

Informa Ltd Registered in England and Wales Registered Number: 1072954

Registered office: Mortimer House, 37-41 Mortimer Street, London W1T 3JH, UK



Advanced Robotics

Publication details, including instructions for authors and subscription information:

<http://www.tandfonline.com/loi/tadr20>

Development of a hyper-redundant multijoint manipulator for maintenance of nuclear reactors

Shugen Ma ^a, Shigeo Hirose ^b & Hiroshi Yoshinada ^c

^a Department of Systems Engineering, Faculty of Engineering, Ibaraki University, 4-12-1 Naka-Narusawa-Cho, Hitachi-Shi 316, Japan

^b Department of Mechano-Aerospace Engineering, Tokyo Institute of Technology, 2-12-1 Ookayama, Meguro-ku, Tokyo 152, Japan

^c Research Division, Komatsu Ltd, Industrial Machinery R&D Center, 1200 Manda, Hiratsuka-Shi, Kanagawa-Ken 254, Japan

Published online: 02 Apr 2012.

To cite this article: Shugen Ma , Shigeo Hirose & Hiroshi Yoshinada (1994) Development of a hyper-redundant multijoint manipulator for maintenance of nuclear reactors, Advanced Robotics, 9:3, 281-300, DOI: [10.1163/156855395X00201](https://doi.org/10.1163/156855395X00201)

To link to this article: <http://dx.doi.org/10.1163/156855395X00201>

PLEASE SCROLL DOWN FOR ARTICLE

Taylor & Francis makes every effort to ensure the accuracy of all the information (the "Content") contained in the publications on our platform. However, Taylor & Francis, our agents, and our licensors make no representations or warranties whatsoever as to the accuracy, completeness, or suitability for any purpose of the Content. Any opinions and views expressed in this publication are the opinions and views of the authors, and are not the views of or endorsed by Taylor & Francis. The accuracy of the Content should not be relied upon and should be independently verified with primary sources of information. Taylor and Francis shall not be liable for any losses, actions, claims, proceedings, demands, costs, expenses, damages, and other liabilities whatsoever or howsoever caused arising directly or indirectly in connection with, in relation to or arising out of the use of the Content.

This article may be used for research, teaching, and private study purposes.
Any substantial or systematic reproduction, redistribution, reselling, loan, sub-
licensing, systematic supply, or distribution in any form to anyone is expressly
forbidden. Terms & Conditions of access and use can be found at [http://
www.tandfonline.com/page/terms-and-conditions](http://www.tandfonline.com/page/terms-and-conditions)

Development of a hyper-redundant multijoint manipulator for maintenance of nuclear reactors

SHUGEN MA, SHIGEO HIROSE* and HIROSHI YOSHINADA†

*Department of Systems Engineering, Faculty of Engineering, Ibaraki University,
4-12-1 Naka-Narusawa-Cho, Hitachi-Shi 316, Japan*

**Department of Mechano-Aerospace Engineering, Tokyo Institute of Technology, 2-12-1 Ookayama,
Meguro-ku, Tokyo 152, Japan*

*†Research Division, Komatsu Ltd, Industrial Machinery R&D Center, 1200 Manda, Hiratsuka-Shi,
Kanagawa-Ken 254, Japan*

Received for AR 25 June 1994

Abstract—A tendon-driven manipulator, the CT Arm, has a specific tendon traction transmission mechanism, in which a pair of tendons for driving a joint is pulled from base actuators via pulleys mounted on the based-side joints. The mechanism makes the most of the coupled drive function of the tendon tractions and thus enables the lightweight manipulator to exhibit enormous payload capability. By this tendon-driven mechanism, a multijoint manipulator with super-redundant degrees of freedom could be realized, which is suitable to the maintenance of nuclear reactors. In this article, we introduce the CT Arm and discuss the possibility of generating a multijoint maintenance manipulator for nuclear reactors, which must have super-redundant degrees of freedom. A position-coordination approach for a hyper-redundant manipulator to carry tools or inspection equipment passing through a hole to a work location in a nuclear reactor is also proposed. Computer simulation has been used to show the validity of the hyper-redundant manipulator and the position-coordination approach for the maintenance of nuclear reactors.

1. INTRODUCTION

A hyper-redundant multijoint manipulator, which behaves like the trunk of an elephant, has unconventional features such as the ability to enter a narrow space while avoiding obstacles. Thus it is suitable for applications where a conventional industrial robot could never be introduced. One of these applications is the maintenance of nuclear reactors.

Most of today's nuclear reactors were not expected to require maintenance of the fixed internal components during their design life time. However, some grades of mild steel exposed to the hottest gas would be oxidizing at unacceptable rates. This oxidation problem provided a strong incentive to carry out research and development work on remotely controlled operations as it is not possible for men to enter the reactor to carry out inspection and remedial work due to the high radiation levels [1–3]. As an example shown in Fig. 1, the maintenance manipulator, which is needed to be

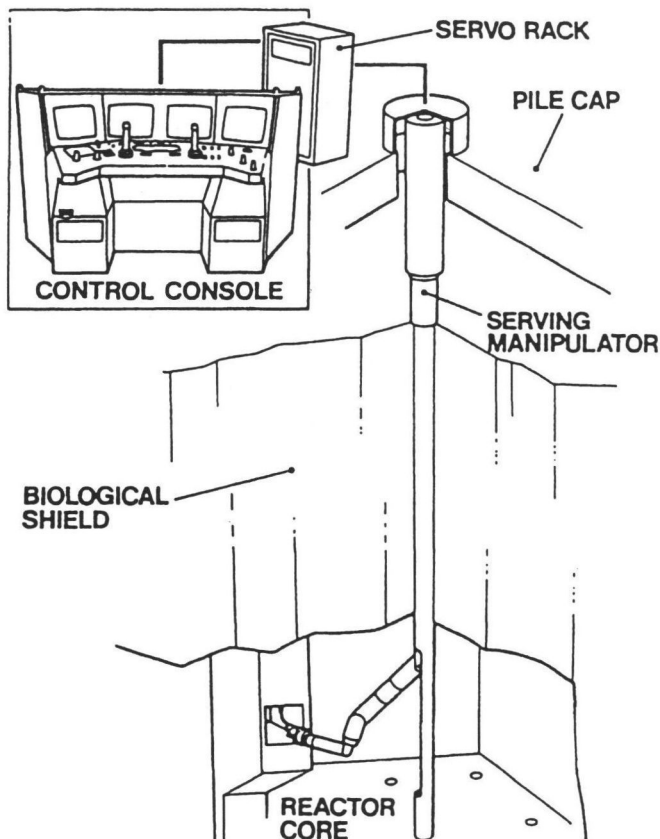


Figure 1. A maintenance manipulator for a gas cooled nuclear reactor.

carry out remote inspection and repair work, can be considered as two distinct parts: the first must be rigid and have sufficient joints and enough reach to get to the work location avoiding any obstacles that may be in the way, and the other must have the dexterity and precision of control to carry out the task. A multijoint manipulator with super-redundant degrees of freedom is a possible candidate to carry tools or inspection equipment to the work location by avoiding obstacles.

However, the realization of such a hyper-redundant multijoint manipulator is difficult because there are serious engineering problems involved. The biggest problem is weight. A multi-degree-of-freedom driving mechanism mounted on the arm makes the manipulator quite heavy. A powerful driving system needed to support such a long and heavy arm makes the arm even heavier. Many mechanisms have so far been proposed to remove the weight restriction, including:

- (1) A lightweight joint design based on a special rotary joint [2–6].
- (2) Provision of a powerful slider at the base to bear as much of the required driving force as possible [7].

- (3) Concentration of the actuators at the base and transmission of the power to each joint through tendons or a special transmission mechanism [8–15].

Despite these efforts, the weight problem has not been overcome for practical use. Therefore, a tendon-driven manipulator named the *CT Arm* has been developed [16, 17], which is based of the coupled drive [18] and the connected differential mechanism [19].

In this paper, we introduce the CT Arm, and discuss the possibility to realize a multijoint maintenance manipulator for nuclear reactors by using the mechanisms of the CT Arm.

The structure of the remainder of the paper is as follows: in Section 2 we will introduce two types of CT Arm mechanism and discuss their advantages over the conventional decoupled mechanism. The effectiveness of the CT Arm will be also demonstrated by a mechanical model (CT ARM-I) in Section 2. In Section 3, we will discuss the possibility to realize a multijoint maintenance manipulator for nuclear reactors which has super-redundant degrees of freedom. A position-coordination algorithm is also introduced in Section 3 for a hyper-redundant manipulator to carry tools or inspection equipment passing in a hole to the work location in a nuclear reactor. The conclusion of the paper is given at Section 4.

2. CT ARM

In this section, we will introduce two types CT Arm mechanisms and a mechanical model: CT ARM-I. Before going into the main topics, we first point out the problems of the conventional decoupled mechanism.

2.1. Problems of the conventional decoupled mechanism

Examples of a multijoint manipulator arm using the conventional decoupled mechanism are illustrated in Fig. 2. The manipulator arms shown are composed of three joints. These belong to the plane mechanism that can be moved within the sagittal plane (*vertical plane parallel to the gravity vector*). These arms are assumed to have a posture to stretch horizontally so that the worst case in terms of gravitational support can be considered. It is supposed that these arms are composed of joints each having L [m] length and uniform weight m [kg] and that a load of M [kg] is held at the tip of the arm. Joints are referred to, respectively, as the i th ($i = 1, \dots, n$) joint from the root towards the tip.

Figure 2(a) shows a commonplace example of a mechanism which has an actuator on each joint. In this construction, torque T_i to be generated by the actuator i is expressed as

$$T_i = (n + 1 - i)MgL + \frac{1}{2}(n + 1 - i)^2mgL. \quad (1)$$

It is known from this equation that a powerful actuator is required for joints close to the root side.

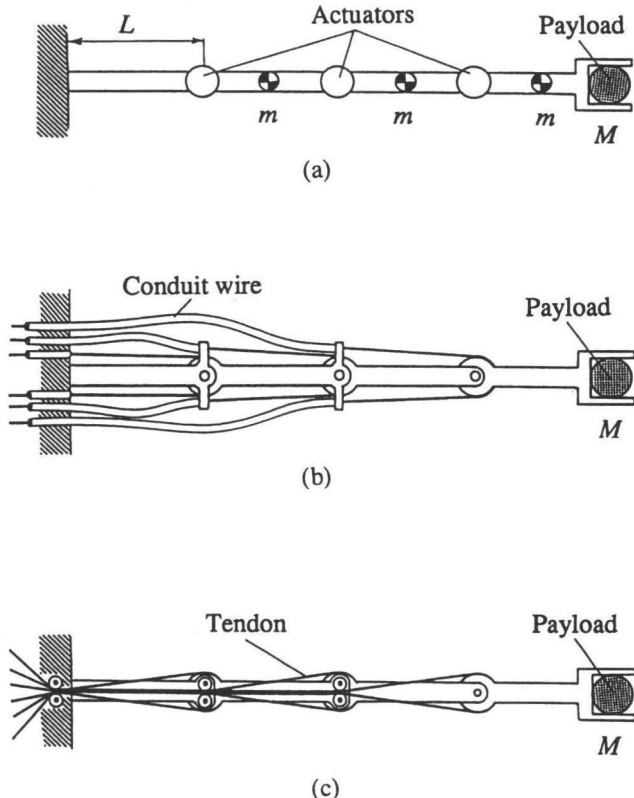


Figure 2. Conventional driving mechanisms for a multijoint manipulator.

Figure 2(b) shows an example where conduit wires are used and each joint is driven remotely by the actuator mounted at the base. Since the arm body is composed of conduit wires and simple mechanisms, this construction reduces weight. However, a large tendon traction force needed to generate the joint torque is still required to drive the root side joints. The tendon traction forces can be described as

$$f_i^{\text{up}} = (n + 1 - i) \frac{MgL}{r} + (n + 1 - i)^2 \frac{mgL}{2r}, \quad (2)$$

$$f_i^{\text{down}} = 0,$$

where r is the radius of the pulleys used at each joint. Friction should also be taken into consideration if generation of a large force by conduit wires is attempted.

Figure 2(c) shows another example where conduit wires are not used, but tendons of the former joints are passed through the center portion of the rear joints, so that the rear will not be affected by tendon traction of the former joints. Because this implementation is free from conduit wires, it is less affected by friction. However, the tendon traction force for driving the joints at the root side is still large.

2.2. Mechanisms of the CT Arm

Before discussing mechanisms of the CT Arm, we first introduce the design concept of the coupled drive [18] and the connected differential mechanism [19].

The coupled drive [18] denotes a mechanism and/or a control system that introduces coupled or cooperated drive of the plural actuators in frequently utilized operation mode and enables higher output power drive. The coupled drive enables us to distribute the output power among the installed actuators. Through the way, the necessary output power for each actuator mounted on robot can be minimized and thus the weight of the whole robot can be reduced. Therefore, it can be said that the coupled drive is the design method which solves the contradictory specifications of introducing multiple degrees of freedom to a robot and lightening the weight of the robot.

The connected differential mechanism [19] is a kind of power distributor which consists of differential mechanisms connected in series. The differential mechanism is the three-port input/output system where one input motion is divided into two output motions. If one of the output ports of the differential mechanism is linked with the input port of the other in series, a system with plural numbers of output ports is eventually created. It gives the possibility to distribute the input power of the single actuator into plural output power without any loss of energy. The soft gripper mechanism shown in Fig. 3 is one example of the connected differential mechanism. In this mechanism, the freely-rotated links are connected in series and the pulleys which can freely rotate around the joint axes are mounted on the joint. The tendon, which is fixed on the tip joint, is wound around the pulleys mounted on each joint with the same wind direction and is to be extended to the base. When the tendon end is pulled, the same torque is applied to each joint of the mechanism in the case of uniform pulley radius (see Appendix). The tendon fraction force is transferred to the torque of all joints. Therefore, the soft gripper is one type of the connected differential mechanism. This mechanism consists of the rotational motion and no sliding motion is included, thus the effect of friction is very small and negligible.

By use of the coupled drive and the connected differential mechanism, the CT Arm, which largely overcomes the mechanical limitations of the conventional decoupled mechanism, can be composed [16]. The basic mechanisms of the CT Arm are shown in Figs 4 and 6. The mechanisms with $n = 3$ are shown here for simplicity.

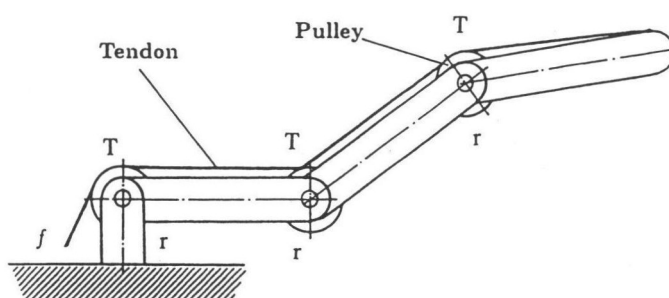


Figure 3. Soft gripper mechanism showing the function of the connected differential mechanism.

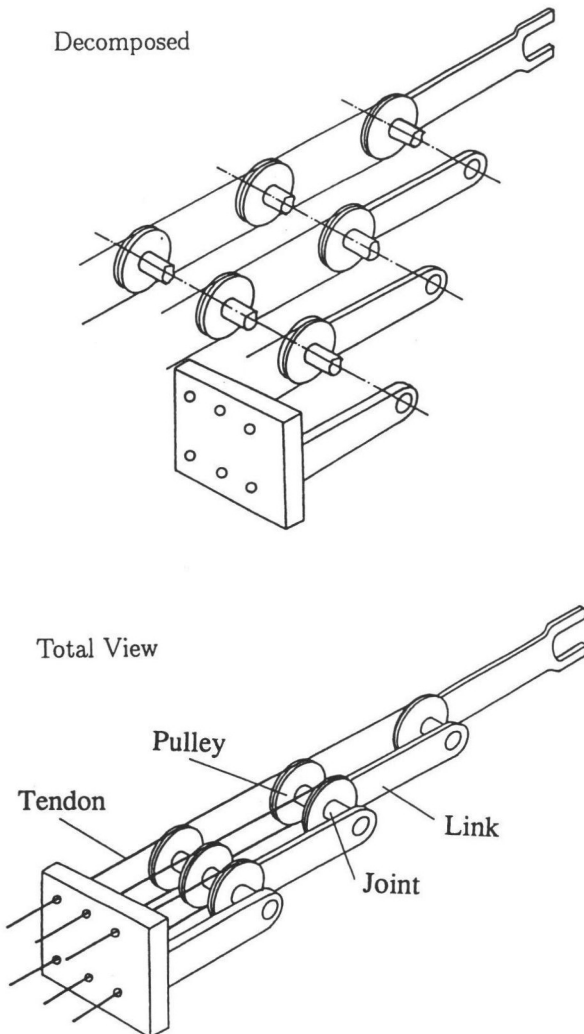


Figure 4. Mechanism of the CT Arm type 1.

2.2.1. CT Arm type 1. Figure 4 shows the CT Arm type 1. The mechanism consists of free connected serial links. One pair of tendons for driving link i ($i = 1, \dots, n$) around joint i is fixed at pulley i , which is riveted on link i while freely rotating around joint i , at one end of them; then they are wound along the way of the pulley of joints $i - 1$ through 1 in the opposite direction, to be extended to the base. The mechanism shown in Fig. 4 is one of the connected differential mechanisms shown in Fig. 3 in which joint power transmission by tendons is employed for each joint. Therefore, when generation of torque T_i at joint i is attempted, the same torque is inevitably generated to joints 1 through $i - 1$ (*in the case of uniform pulley radius*). As far as joint i is connected, power transmission pulleys to drive joints $i + 1, \dots, n$ of the tip side are pivoted to this joint and therefore torques produced to drive these

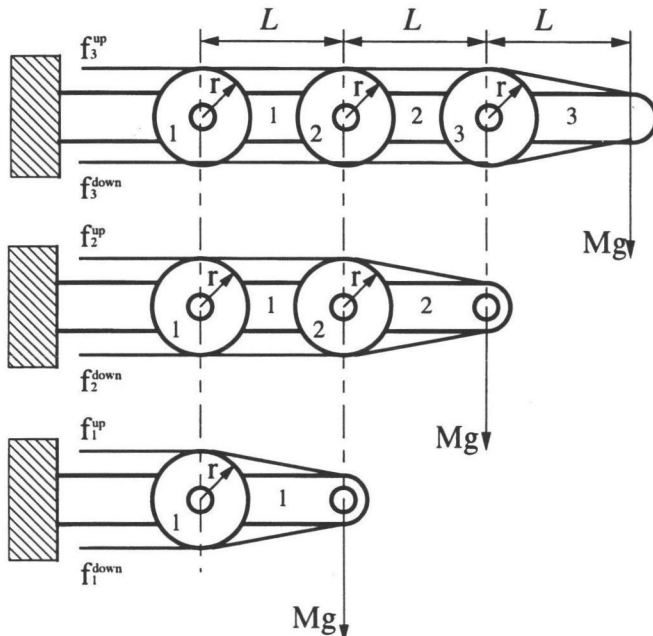
joints are accumulated at joint i . In other words, in contrast to the conventional mechanisms shown in Fig. 2, the effect of the coupled drive is positively used in the mechanism of Fig. 4.

The tendon traction forces to drive joint i of the CT Arm type 1 in the arm configuration of Fig. 4 can be expressed as (see Fig. 5):

$$f_i^{\text{up}} = \frac{MgL}{r} + \left(n + \frac{1}{2} - i \right) \frac{mgL}{r}, \quad (3)$$

$$f_i^{\text{down}} = 0.$$

Let the tendon fraction forces of equation (3) be compared with those equation (2) to quantitatively investigate the meanings of the mechanism introduced here. In equation (2), the traction force to support tip payload Mg at joint n is MgL/r . This increases in proportion to the decrease of joint number. On the other hand, in equation (3), the supporting traction force of the payload Mg remains at a constant value of MgL/r at every joint, as shown by the first term of the right side. This is because the tendon traction forces are coupled positively.



In the case of the zero arm weight,

$$f_3^{\text{up}} = MgL/r, \quad f_3^{\text{down}} = 0$$

$$f_2^{\text{up}} = MgL/r, \quad f_2^{\text{down}} = 0$$

$$f_1^{\text{up}} = MgL/r, \quad f_1^{\text{down}} = 0$$

Figure 5. Tendon traction forces at the CT Arm type 1.

As for the tendon traction force supporting the arm's own weight, it is proportional to the square of the number of joints in equation (2). In equation (3), however, it is linearly increased, as shown by the second term on the right side. As shown here, the CT Arm reduces the burden of the tendon traction force remarkably.

2.2.2. CT Arm type 2. Figure 6 shows CT Arm type 2. The basic construction of this mechanism is the same as that of type 1. The only difference is that a pair of tendons to drive a certain joint i are passed through joints $n - 1$ to 1, where two pulleys are provided, and both tendons are stretched on the same side of the pulleys. All driving tendons are designed to stretch on one side of the manipulator. The tendon-stretched side is always controlled so as to be positioned at the upper side of the arm with regard to gravity.

CT Arm type 2 has the characteristic that the traction of both pairs of tendons can effectively be used for coupled drive. To clarify this point, let us assume a traction control where torque T_i is generated at joint i by the difference of traction force between a pair of tendons while bias force $f_{0(i)}$ is applied to the same pair of

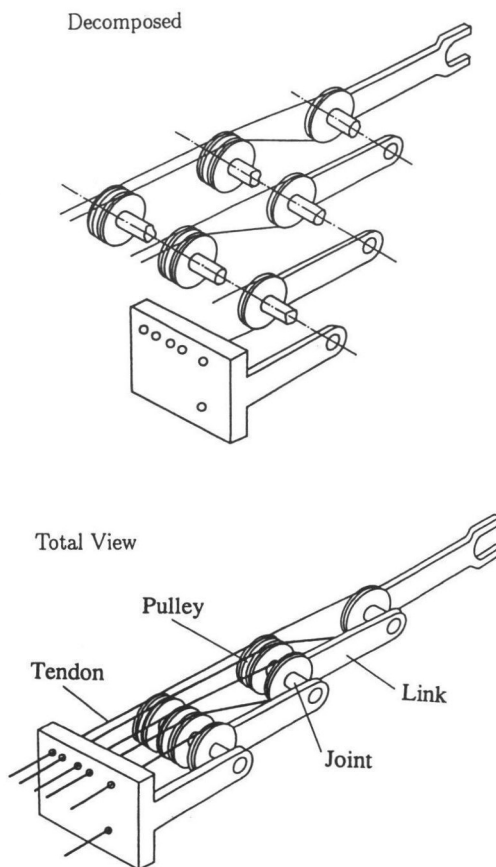


Figure 6. Mechanism of the CT Arm type 2.

tendons. In the case of the type 1 mechanism, application of bias force $f_{0(i)}$ does not change the resultant torque of joints $1, \dots, i$. However, in the case of the type 2 mechanism, the torque due to bias force $2f_{0(i)}$ of tendons is added to the torque of root joints $1, \dots, i-1$ in addition to torque T_i even though the torque of joint i has been maintained as T_i . If the tendon-stretched side of the arm is always maintained at the upper side with regard to gravity, this torque, which is produced by bias force, can be used to sustain the weight of the payload and the manipulator itself. Therefore, fuller use is made of the coupled drive.

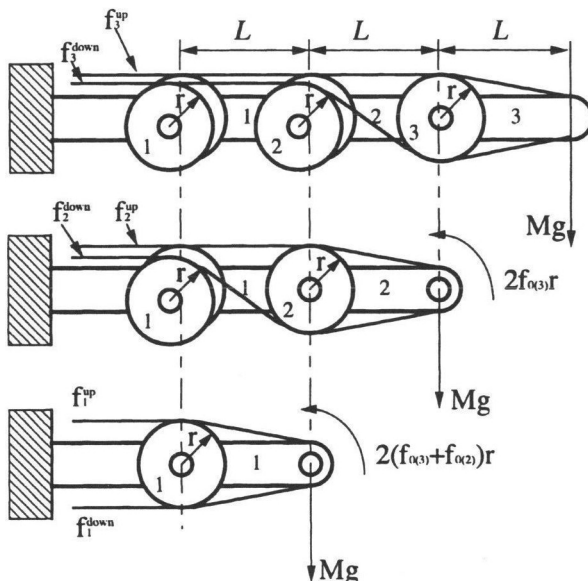
This effectiveness is shown through the example of Fig. 6. In the case of the mechanism shown in Fig. 6, the tendon traction forces to generate the supporting torque T_i for joint i , are expressed as (see Fig. 7)

$$f_i^{\text{up}} = f_{0(i)} + \frac{MgL}{r} + \left(n + \frac{1}{2} - i\right) \frac{mgL}{r} - 2 \sum_{k=i+1}^n f_{0(k)}, \quad (4)$$

$$f_i^{\text{down}} = f_{0(i)},$$

in the arm configuration of Fig. 6.

It is considered from this that the tendon traction forces to generate the joint torque for the joint at the root side are further reduced by the effect of bias force interference.



In the case of the zero arm weight,

$$\begin{aligned} f_3^{\text{up}} &= MgL/r + f_{0(3)}, & f_3^{\text{down}} &= f_{0(3)} \\ f_2^{\text{up}} &= MgL/r + f_{0(2)} - 2f_{0(3)}, & f_2^{\text{down}} &= f_{0(2)} \\ f_1^{\text{up}} &= MgL/r + f_{0(1)} - 2f_{0(2)} - 2f_{0(3)}, & f_1^{\text{down}} &= f_{0(1)} \end{aligned}$$

Figure 7. Tendon traction forces at the CT Arm type 2.

2.3. Mechanical model: CT ARM-I

In order to show the effectiveness of the CT Arm, a mechanical model of the CT Arm, named *CT ARM-I*, had been developed, as shown in Fig. 8 [17]. Figure 8 only shows the type 1 CT Arm, the type 2 CT Arm can easily be constructed by changing the direction in which the tendon is stretched. The CT ARM-I has all 9 d.o.f. (*including one 1 d.o.f. in gripper and 1 degree of swinging freedom in the base of the arm*); the length of the entire arm is about 1.2 m and the total arm weight is about 21 kg. All parameters of the CT ARM-I, which are shown in Fig. 9, are listed in Table 1.

The joints of the CT ARM-I are driven by 16 base-mounted 100 W torque-control DC servo-motors through tendons and pulleys, and the entire arm is rotated by a 100 W velocity-control DC servo-motor. (The electrohydraulic system is generally considered the better driving system for the CT ARM-I than the DC servo-motor system. The reason that we select the DC servo-motor system is the easy management and the enormous knowledge about the DC servo-motor system. First needs are to know about the characteristics about the mechanism of the CT Arm, not the properties about the driving system. The discussion about the driving system will be executed in future articles.) Potentiometers mounted on every joint are used to measure the joint angles, tachometers mounted on each motor are used to measure the joint velocity and the tendon tractions are measured by means of a miniature strain-gage tendon traction sensor unit. Table 2 shows all the components of the driving and sensing parts which have been used in the CT ARM-I.

Preliminary tests on the CT ARM-I confirmed the excellence of its basic movement performance and the following characteristics were demonstrated.

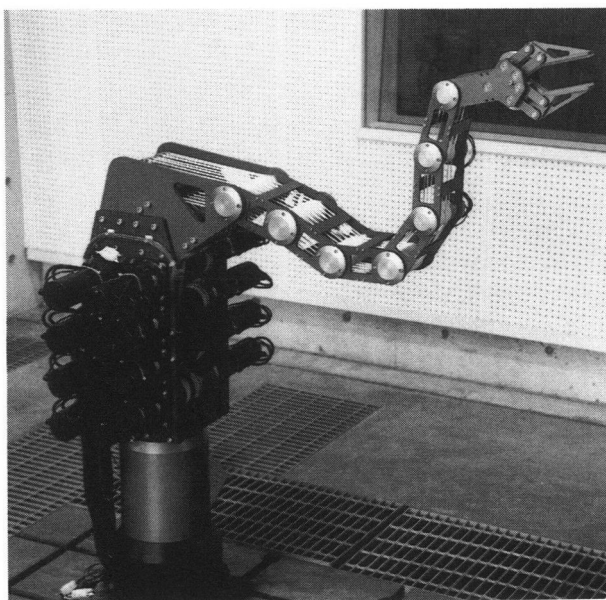


Figure 8. Overall view of the CT ARM-I.

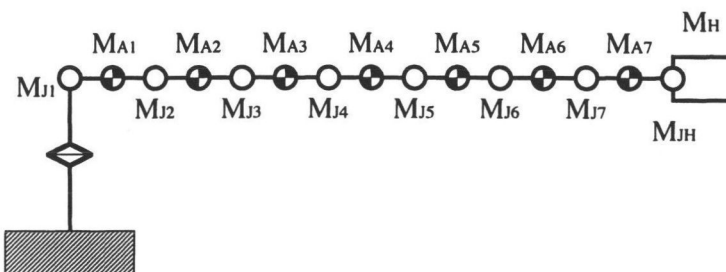


Figure 9. Arm parameters of the CT ARM-I.

Table 1.
Parameters of the CT ARM-I

Mass of joint (kg)	Mass of arm (kg)	Diameter of pulley (mm)		Length of arm (mm)	
M _{J1} 3.27	M _{A1} 0.70	D _{P1}	60	L ₁	150
M _{J2} 2.93	M _{A2} 0.67	D _{P2}	60	L ₂	150
M _{J3} 2.55	M _{A3} 0.62	D _{P3}	60	L ₃	150
M _{J4} 2.34	M _{A4} 0.45	D _{P4}	60	L ₄	150
M _{J5} 1.72	M _{A5} 0.40	D _{P5}	50	L ₅	150
M _{J6} 1.58	M _{A6} 0.38	D _{P6}	50	L ₆	150
M _{J7} 1.49	M _{A7} 0.49	D _{P7}	50	L ₇	150
Mass of hand driving part (kg)	Mass of hand (kg)	Diameter of hand driving pulley (mm)		Length of hand (mm)	
M _{JH} 1.14	M _H 1.01	D _{PH}	50	L _H	150
Diameter of pulley mounted on the motors D _{Pmotor} (mm)		80			

Table 2.
Elements used in the CT ARM-I

Driving part	actuator	joints and gripper: 100 W torque-control DC servo-motor
		whole arm rotation: 100 W velocity-control DC servo-motor
reduction gear		harmonic drive (1/100)
tendon		Kelvar code (limited traction 3500 N, diameter 3.0 mm)
Sensing part	angle sensor	potentiometer
	velocity sensor	tachometer
	tendon traction sensor	miniature strain-gain tendon traction sensor unit

2.3.1. Large payload capability. One characteristic of the CT ARM-I is that of enormous payload capabilities. Comparison of the payload capability of the CT ARM-I with that of traditional decoupled multijoint manipulators has shown that the CT ARM-I can exhibit a higher payload capability.

In the case of the CT ARM-I type 1, a payload of about 3.4 kg could be lifted while the arm is stretched horizontally (*the worst case in terms of gravitational support*); CT ARM-I type 2 can lift a payload of about 8 kg at the worst case in terms of gravitational support. However, if the same driving system and mechanism as those in the CT ARM-I are used in the traditional design, where the driving system is not coupled or interfered with, not even the weight of the arm itself can be supported. Therefore, it is clearly demonstrated that the CT ARM-I has much better payload capability.

2.3.2. Variable compliance arm structure. Every joint of the CT ARM-I is driven by two actuators through the tendon having non-linear stiffness; thus the stiffness of the joint can be adjusted by controlling the bias traction force of the tendon between these two actuators. Therefore, the compliance of the arm can be adjusted for each industrial task through control of the actuators, meaning that the desired arm compliance corresponding to the work to be performed can easily be obtained.

3. A MULTIJOINT MAINTENANCE MANIPULATOR FOR NUCLEAR REACTORS

As stated in the Introduction, the maintenance manipulator for nuclear reactors must have sufficient joints and degrees of freedom, as well as enough reach to get to the work location while avoiding any obstacles (see Fig. 1). A multijoint manipulator with super-redundant degrees of freedom is capable of being used for maintenance of nuclear reactors, while its weight problem can be overcome (*it can be solved by the CT Arm mechanism mentioned in the Section 2*).

In the mechanisms of the CT Arm, the tendon traction for lifting a payload does not concentrate on one actuator, but is distributed among all actuators. Thus, the payload capability of the CT Arm is not limited by the output of one actuator, but by the summary output of all actuators, and thus can be much larger. Therefore, the mechanisms of the CT Arm enable the lightweight manipulator to exhibit enormous payload capability. This was also demonstrated by the CT ARM-I. As a result, we know that the mechanisms of the CT Arm make it possible to realize a multijoint maintenance manipulator for nuclear reactors which has super-redundant degrees of freedom.

A hyper-redundant multijoint manipulator for the maintenance of nuclear reactors could be generated by the CT Arm mechanisms. However, because of the kinematic redundancy between the end-effector and the joints, and the static redundancy between the tendons and the joints, the hyper-redundant manipulator will not exhibit its power for maintenance in nuclear reactors unless an appropriate control system can be supplied. In this article, a real-time position-coordination algorithm to resolve the

kinematic redundancy is introduced on the basis of curvilinear theory. The decoupling algorithm to decouple the interference between the tendons and to resolve the static redundancy will be discussed in future articles; however, the basic idea of the approach can be found elsewhere [16].

3.1. Curvilinear treatment of a hyper-redundant manipulator

The algorithm for the position-coordination of a hyper-redundant manipulator was introduced to resolve its kinematic redundancy by many researchers [20–22]. However, a position-coordination algorithm concentrated on the maintenance of nuclear reactors was not fully discussed; it will, however, be treated in this paper. To compose a real-time coordination algorithm, the continuous curvilinear theory is used to resolve the super-redundancy, not the conventional algebraic strategies (*vector and matrix theory*).

Continuous curvilinear theory models the posture of a hyper-redundant manipulator arm with the curvature function $\kappa(s)$, which represents the curvature of the arm at distance s along the curve measured from the base (see Fig. 10).

For example, the curvature function

$$\kappa(s) = \text{const} \quad (5)$$

generates a circular curve, while the curvature function

$$\kappa(s) = ks, \quad (6)$$

where k is constant scalar, generates a clothoid spiral.

The serpenoid curve, which is defined for the snake wave motion [22], is better used to define the arm posture of hyper-redundant manipulators, because of the easily obtained inverse solution from the given boundary position and the length of curve to the structure of curve, in the case that we define the solution of boundary position derived from the known curve structure as direct solution. The curvature of the serpenoid curve was defined by the sine function [20].

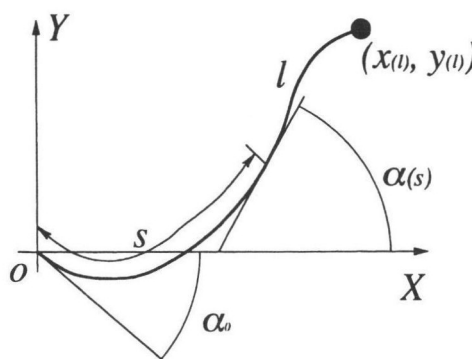


Figure 10. Specification of the curve parameters.

Consider a serpenoid curve, the curvature of which is defined as

$$\kappa(s) = \frac{2\pi}{l} a_1 \cos\left(\frac{2\pi}{l} s\right) + \frac{2\pi}{l} a_2 \sin\left(\frac{2\pi}{l} s\right), \quad (7)$$

where l is the curve length which is equal to the length of the manipulator arm that is to be configured. The angle $\alpha(s)$, which represents the inclination angle of the vector in relation to the x -axis on the curvilinear length s , and the position of $x-y$ coordinates $(x(s), y(s))$ at the stated position can be derived and obtained by

$$\alpha(s) = \int_0^s \kappa(z) dz = a_1 \sin\left(\frac{2\pi}{l} s\right) + a_2 \left[1 - \cos\left(\frac{2\pi}{l} s\right)\right] + \alpha_0, \quad (8)$$

$$\begin{aligned} x(s) &= \int_0^s \cos(\alpha(z)) dz \\ &= \cos(a_0 + a_2) \int_0^s \cos\left(a_1 \sin\left(\frac{2\pi}{l} z\right) - \cos\left(\frac{2\pi}{l} z\right)\right) dz \\ &\quad - \sin(a_0 + a_2) \int_0^s \sin\left(a_1 \sin\left(\frac{2\pi}{l} z\right) - \cos\left(\frac{2\pi}{l} z\right)\right) dz, \end{aligned} \quad (9)$$

$$\begin{aligned} y(s) &= \int_0^s \sin(\alpha(z)) dz \\ &= \sin(a_0 + a_2) \int_0^s \cos\left(a_1 \sin\left(\frac{2\pi}{l} z\right) - \cos\left(\frac{2\pi}{l} z\right)\right) dz \\ &\quad + \cos(a_0 + a_2) \int_0^s \sin\left(a_1 \sin\left(\frac{2\pi}{l} z\right) - \cos\left(\frac{2\pi}{l} z\right)\right) dz. \end{aligned} \quad (10)$$

In the case that $s = l$, the end position of the curve can be given by

$$\begin{aligned} x(l) &= \cos(a_0 + a_2) J_0\left(\sqrt{a_1^2 + a_2^2}\right) l, \\ y(l) &= \sin(a_0 + a_2) J_0\left(\sqrt{a_1^2 + a_2^2}\right) l, \end{aligned} \quad (11)$$

where J_0 is the zero-order Bessel function [23].

While the end position of the curve is given, its structure given by the curvature function $\kappa(s)$ can be defined by deriving the coefficients a_1 and a_2 . The coefficients a_1 and a_2 are obtained by inverting equation (11), and are given by

$$\begin{aligned} a_2 &= \tan^{-1}\left(\frac{y(l)}{x(l)}\right) - \alpha_0, \\ a_1 &= \left(\left[J_0^{-1} \left\{ (x(l)^2 + y(l)^2)^{1/2} / l \right\} \right]^2 - \left\{ \tan^{-1}\left(\frac{y(l)}{x(l)}\right) - \alpha_0 \right\}^2 \right)^{1/2}, \end{aligned} \quad (12)$$

where J_0^{-1} is the restricted inverse zero-order Bessel function [23]. Thus, the inverse solution of the curve (*the structure of the curve*) is derived and defined by the coefficients a_1 and a_2 . The manipulator arm posture can be configured by restricting the arm on the serpenoid curve. In this case, the joint angles are derived from the grade of the tangent line as

$$\begin{aligned} q_1 &= \alpha\left(\frac{1}{2} L\right) = \alpha\left(\frac{1}{2N} l\right), \\ q_i &= \alpha\left(\frac{i}{2} L\right) - \alpha\left(\frac{i-1}{2} L\right) = \alpha\left(\frac{i}{2N} l\right) - \alpha\left(\frac{i-1}{2N} l\right), \quad i = 2, 3, \dots, N. \end{aligned} \quad (13)$$

where N is the joint number of the manipulator to be configured and L is the length of the link, equal to l/N . This discrete method through which the discrete manipulator arm is restricted to the continuous curve makes the position error of the end position of the manipulator smaller than 10^{-6} and the position error of each joint smaller than 0.01 [24]. Therefore, the joint angles of the manipulator arm to be configured can be obtained by substituting equation (8) into equation (13) and expressed as

$$\begin{aligned} q_1 &= a_1 \sin \frac{\pi}{N} + a_2 \left(1 - \cos \frac{\pi}{N}\right) + \alpha_0, \\ q_i &= a_1 \left[\sin \left(\frac{2\pi}{N} i\right) - \sin \left(\frac{2\pi}{N} (i-1)\right) \right] \\ &\quad - a_2 \left[\cos \left(\frac{2\pi}{N} i\right) - \cos \left(\frac{2\pi}{N} (i-1)\right) \right], \quad i = 2, 3, \dots, N. \end{aligned} \quad (14)$$

As a result, the inverse kinematic solution, in which the joint angles of the manipulator that needs to be configured are derived from the given end position ($x(l)$, $y(l)$), has been derived by equations (12) and (14).

3.2. A maintenance manipulator to carry tools or inspection equipment passing through a hole to the work location in a nuclear reactor

On the basis of the above-stated manipulator coordination technique, a hyper-redundant maintenance manipulator can easily carry out work in which tools or inspection equipment needs to be brought to the work location while avoiding obstacles in the nuclear reactor. An example where the manipulator arm passes through a hole is used to show the validity of the hyper-redundant multijoint manipulator and the introduced position-coordination algorithm for the maintenance of nuclear reactors.

The maintenance manipulator that passes into a hole (*or a pipe*) is divided two parts. One part is in the hole (*or pipe*), which has the length $l_{in} = \int_0^t v(z) dz$ (where $v(t)$ is the driving speed along the center of the hole). Another part is at the outside of the hole, whose length is given by $l_{out} = l_{whole} - l_{in}$ (where l_{whole} is the whole length of the manipulator arm). The part of the manipulator arm in the hole is driven along the center of the hole with a slow speed $v(t)$, but the outside part of the manipulator is configured to a continuous curve by the technique stated in Subsection 3.1. In

order for the manipulator arm to be easily pushed into the hole, the orientation of the outside part of the manipulator at the entrance of the hole must coincide with the center line of the hole. Thus, the outside part of the manipulator can be configured out by setting the length $l = l_{\text{out}}$ and the inclination angle $\alpha_0 = \phi_{\text{hole}}$ (ϕ_{hole} is the inclination angle of the hole at the entrance) in equations (12) and (14). That is,

$$\begin{aligned} a_2 &= \tan^{-1} \left(\frac{y(l_{\text{out}})}{x(l_{\text{out}})} \right) - \phi_{\text{hole}}, \\ a_1 &= \left(\left[J_0^{-1} \left\{ (x(l_{\text{out}})^2 + y(l_{\text{out}})^2)^{1/2} / l_{\text{out}} \right\} \right]^2 \right. \\ &\quad \left. - \left\{ \tan^{-1} \left(\frac{y(l_{\text{out}})}{x(l_{\text{out}})} \right) - \phi_{\text{hole}} \right\}^2 \right)^{1/2}; \end{aligned} \quad (15)$$

$$\begin{aligned} q_1 &= a_1 \sin \frac{\pi}{N} + a_2 \left(1 - \cos \frac{\pi}{N} \right) + \phi_{\text{hole}}, \\ q_i &= a_1 \left[\sin \left(\frac{2\pi}{N} i \right) - \sin \left(\frac{2\pi}{N} (i-1) \right) \right] \\ &\quad - a_2 \left[\cos \left(\frac{2\pi}{N} i \right) - \cos \left(\frac{2\pi}{N} (i-1) \right) \right], \quad i = 2, 3, \dots, N, \end{aligned} \quad (16)$$

where $N = l_{\text{out}}/L$. On the other hand, the inside part of the manipulator is easily configured and the joint angles are easily derived by setting this part of the manipulator arm on the center line of the hole.

Figure 11 shows an example where the hyper-redundant multijoint manipulator with 30 d.o.f. passes through a hole. As seen, the part of the manipulator in the hole

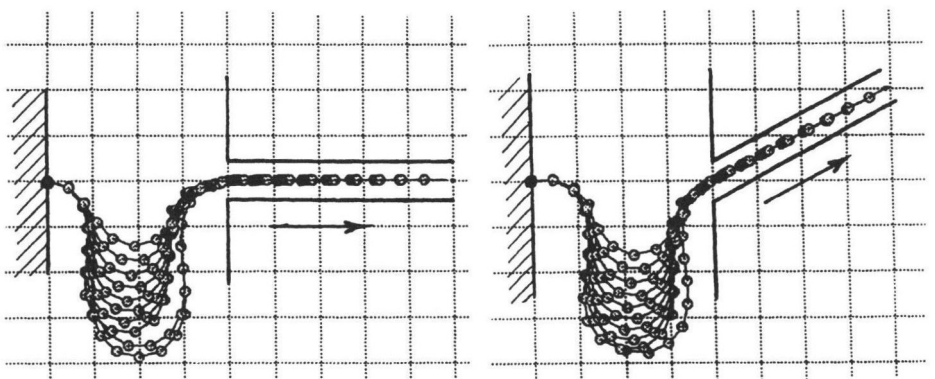


Figure 11. Examples to show that a hyper-redundant multijoint manipulator passes in a hole.

(or pipe) is driven along the center of the hole (or pipe), but the outside part of the manipulator is well configured to the continuous curve (*surpenoid curve*).

4. CONCLUSION

In this paper, we have introduced the CT Arm mechanisms and demonstrated its effectiveness by a mechanical model: CT ARM-I. The CT Arm is based on the design concept of the coupled drive and the connected differential mechanism, and thus the tendon traction for lifting a payload does not concentrate on one actuator, but is distributed among all actuators. Therefore, the payload capability of the CT Arm is not limited by the output of one actuator, but by the summary output of several actuators, and can thus be much larger. In addition, every joint of the CT Arm is driven by two actuators, meaning that the desired arm compliance corresponding to the work to be performed can easily be obtained by adjusting the bias traction force of the tendon.

As a result, we know that the mechanisms of the CT Arm make it possible to realize a multijoint maintenance manipulator for the maintenance of nuclear reactors. In addition, a position-coordination algorithm was introduced to fully utilize the hyper-redundant manipulator for nuclear reactor maintenance. An example been used to show that the proposed algorithm can guarantee that the hyper-redundant manipulator executes the given maintenance work in a nuclear reactor.

Acknowledgements

Special thanks to Toshihisa Naruse (Senior Manager, Komatsu Ltd) for his support. The authors also thank Tatsunori Suwa (Komatsu Ltd) for his help.

REFERENCES

1. D. W. Perrat, "Remote operations inside nuclear reactors," in *Proc. 1987 Remote Systems and Robotics in Hostile Environments*, Pasco, Washington, 1987, pp. 182–189.
2. K. Asano, M. Obama, Y. Arimura, M. Kondo and Y. Hitomi, "Multijoint inspection robot," *IEEE Trans. Industrial Electronics*, vol. IE-30, no. 3, pp. 277–281, 1983.
3. M. Obama, F. Ozaki and K. Asano, "A locomotive inspection of robot for turbine building interior inspection in nuclear power plants," in *Proc. 1985 Int. Conf. on Advanced Robotics*, Tokyo, Japan, 1985, pp. 355–362.
4. S. Hirose, S. Oda and Y. Umetani, "An active cord mechanism with oblique swivel joints and its control," in *Proc. 1981 ROMANSY*, Zaborów near Warsaw, Poland, 1981, pp. 395–407.
5. H. J. Taylor, "A large-scale manipulator for shuttle payload handling," in *Proc. 26th Conf. on Remote System Technology*, 1978, p. 90.
6. Y. Nakahara, "The development of an extensible elephant's nose type arm," in *Proc. 1987 Annual Conf. SICE*, Hiroshima, Japan, 1987, pp. 595–596 (in Japanese).
7. S. Hirose and S. Ma, "Moray drive for multijoint manipulators," *J. Robotics Soc. Jpn.*, vol. 8, no. 1, pp. 9–16, 1990 (in Japanese); and in *Proc. 5th Int. Conf. on Advanced Robotics*, vol. 1, pp. 521–526, Pisa, Italy, 1991.
8. V. V. Anderson and R. C. Horn, "Tenser arm manipulator design," *ASME Trans.*, vol. 67-DE-57, pp. 1–12, 1967.

9. W. K. Taylor, D. Lavie and I. I. Esat, "A curvilinear snake arm robot with gripper-axis fiber-optic image processor feedback," *Int. J. Robotica*, vol. 1, pp. 33–39, 1983.
10. S. Hirose, T. Kado and Y. Umetani, "Tenser actuated elastic manipulator," *Proc. 6th IFToMM World Congress*, vol. 2, pp. 978–981, New Delhi, India, 1983.
11. A. Hemani, "Studies on a light weight and flexible robot manipulator," *Int. J. Robotica*, vol. 1, pp. 27–36, 1985.
12. M. Wada, Y. Kuba and S. Nishihara, "Design of flexible multijoint manipulator," in *Proc. 1984 Annual Conf. SICE*, Tokyo, Japan, 1984, pp. 359–360.
13. S. C. Jacobsen, J. E. Wood, D. F. Knutti and K. B. Biggers, "Design of the Utah/MIT dexterous hand work in progress," *Int. J. Robotics Res.*, vol. 4, no. 3, pp. 21–50, 1986.
14. S. C. Jacobsen, E. K. Iversen, D. F. Knutti, R. T. Johnson and K. B. Biggers, "Design of the Utah/MIT dexterous hand," *Proc. 1986 IEEE Int. Conf. on Robotics and Automation*, vol. 3, pp. 1520–1534, San Francisco, CA, 1986.
15. D. D. Ardayfio, *Fundamentals of robotics*. New York: Marcel Dekker, 1987, pp. 34–44.
16. S. Hirose and S. Ma, "Coupled tendon-driven multijoint manipulator," *Proc. 1991 IEEE Int. Conf. on Robotics and Automation*, vol. 2, pp. 1268–1275, Sacramento, CA, 1991.
17. S. Ma, S. Hirose and H. Yoshinada, "CT Arm-I: coupled tendon-driven manipulator model I – design and basic experiment," *Proc. 1992 IEEE Int. Conf. on Robotics and Automation*, vol. 3, pp. 2094–2100, Nice, France, 1992.
18. S. Hirose and M. Sato, "Coupled drive of the multi-DOF robot," *1989 IEEE Int. Conf. on Robotics and Automation*, vol. 3, pp. 1610–1616, Scottsdale, AZ, 1989.
19. S. Hirose, "Connected differential mechanism and its application," in *Proc. 1985 Int. Conf. on Advanced Robotics*, Tokyo, Japan, 1985, pp. 319–329.
20. S. Hirose, K. Yokoshima and S. Ma, "2-DOF Moray Drive for Hyper-Redundant Manipulators," *Proc. 1992 Int. Conf. on Intelligent Robots and Systems*, vol. 3, pp. 1753–1740B, Raleigh, NC, 1992.
21. G. S. Chirikjian and J. W. Burdick, "An obstacle avoidance algorithm for hyper-redundant manipulators," *Proc. 1990 Int. Conf. on Robotics and Automation*, vol. 1, pp. 625–631, Cincinnati, OH, 1990.
22. S. Hirose, *Biologically Inspired Robots*. Oxford, Oxford University Press, 1993.
23. I. N. Sneddon, *Special Functions of Mathematical — Physics and Chemistry*. London: Oliver & Boyd, 1961.
24. K. Yokoshima, *Study on the Control of the Moray-drive type Multijoint Manipulator*. ME Dissertation, Department of Mechanical Engineering Science, Tokyo Institute of Technology, 1992.

APPENDIX

The connected differential mechanism (*or soft gripper mechanism*) has a property that the tendon traction generates the same torque at each joint in the case of pulleys of the same radius.

Generally, the torques for supporting the payload Mg is given by

$$T_1 = 3MgL, \quad T_2 = 2MgL, \quad T_3 = MgL. \quad (\text{A1})$$

In Fig. A1, while the tendon traction f has the value of MgL/r , link 3 can be supported by the torque generated by this tendon traction. However, the torque generated only by the tendon traction is not big enough to support links 1 and 2, the other torques $T_1 = 2MgL$, $T_2 = MgL$ must be added to support links 1 and 2. The torques for supporting links 1 and 2 are the addition of the torques generated by the tendon traction f and the torques T_1 and T_2 . Therefore, besides the torques $T_1 = 2MgL$, $T_2 = MgL$, the same torque MgL at joints 1 and 2 as that at joint 3 must be generated by the tendon traction f to support all links. That is, the tendon traction generates the same torques at each joint, in the case of the same pulley radius at each joint.

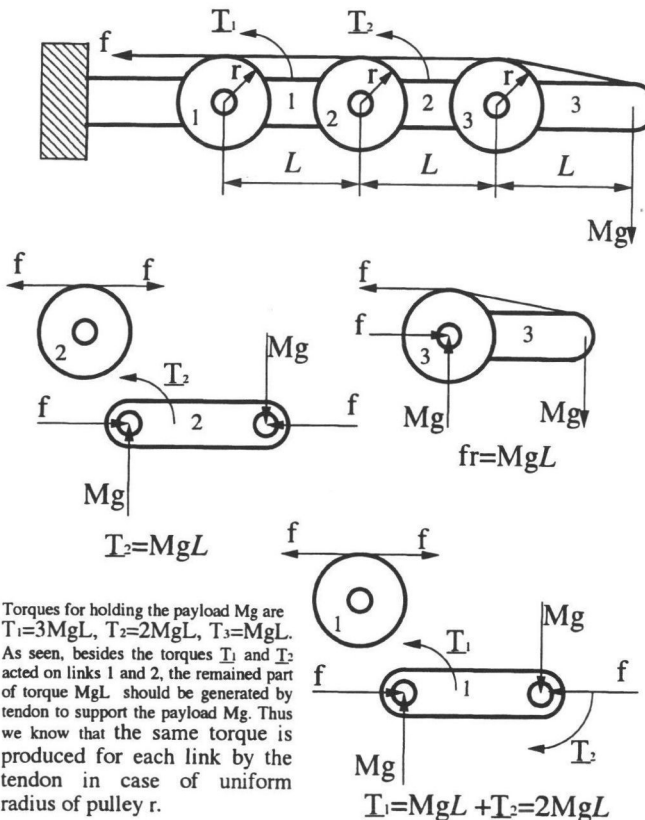


Figure A1. Tendon traction force and the joint torques at the soft gripper mechanism.

ABOUT THE AUTHORS



Shugen Ma was born in China in 1963. He received the BEng degree (first class honours) in Mechanical Engineering from Hebei Institute of Technology, China in 1984. He then went on to receive his MEng and DrEng degrees in Mechanical Engineering Science from Tokyo Institute of Technology (Japan) in 1988 and 1991, respectively. From 1991 to 1992 he worked for Komatsu Ltd as a Research Engineer, and from 1992 to 1993 he was at University of California Riverside (USA) as a Visiting Scholar. Since July 1993 he has been with Ibaraki University (Japan), Faculty of Engineering, as an Assistant Professor. His research interest is in the design and control theory of new types of robots, the mechanism and control of redundant manipulators, and the distributed robot system. He was awarded the Outstanding Paper prize from SICE in 1992. He is a member of the Robotics Society of Japan, SICE, JSME and the IEEE.



Shigeo Hirose was born in Tokyo in 1947. He received the BEng degree (first class honours) in Mechanical Engineering from Yokohama National University in 1971, MEng and DrEng degrees in Control Engineering from Tokyo Institute of Technology in 1973 and 1976, respectively. From 1976 to 1979 he was Research Associate, from 1979 to 1992 he was Associate Professor and from 1992 he has been Professor of the Department of Mechano-Aerospace Engineering, Tokyo Institute of Technology. His research interest is in the design of mechanisms, sensors and control systems of novel robotic systems, e.g. snake-like articulated body mobile robots and manipulators, quadruped walking robots, terrain adaptive vehicles and wall climbing robots. He has been awarded 15 prizes for his academic achievement, papers and publications; from the Society of Instrument of Control Engineers in 1976, 1983, 1989 and 1992; from the Robotics Society of Japan in 1987, 1992 and 1993; from Japanese Society of Mechanical Engineers in 1971 and 1994; from a Japan Industrial Robot Association in 1990 and 1992; and so on. He has published more than 160 academic papers and several books including *Snake Inspired Robots* from Kogyo-chosakai Publishing in 1987 (in Japanese), *Robotics* from Shokabo Publishing in 1987 (in Japanese) and *Biologically Inspired Robots* from Oxford University Press in 1993.



Hiroshi Yoshinada received the BE and ME degrees in mechanical engineering science from Tokyo Institute of Technology in 1976 and 1978, respectively. Since 1978, he has been with Komatsu Ltd, Hiratsuka, Kanagawa, Japan, where he is a chief research manager, Industrial Robotics Group, Research Division. His research interests are in the design and control theory of manipulators, teleoperation and underwater robotics. He is a member of the Japan Society of Mechanical Engineers and the Robotics Society of Japan.